The integer quantum Hall effect of a square lattice with an array of point defects

2012 J. Phys.: Condens. Matter 24 345501

(http://iopscience.iop.org/0953-8984/24/34/345501)

IOP PUBLISHING JOURNAL OF PHYSICS: CONDENSED MATTER

J. Phys.: Condens. Matter **24** (2012) 345501 (12pp) doi:10.1088/0953-8984/24/34/345501

The integer quantum Hall effect of a square lattice with an array of point defects

S İslamoğlu, M Ö Oktel and O Gülseren

Department of Physics, Bilkent University, 06800 Ankara, Turkey

E-mail: selcen@fen.bilkent.edu.tr, oktel@fen.bilkent.edu.tr and gulseren@fen.bilkent.edu.tr

Received 23 March 2012, in final form 29 June 2012
Published 31 July 2012
Online at stacks.iop.org/JPhysCM/24/345501

Abstract

The electronic properties of a square lattice under an applied perpendicular magnetic field in the presence of impurities or vacancies are investigated by the tight-binding method including up to second nearest neighbor interactions. These imperfections result in new gaps and bands in the Hofstadter butterfly even when the second order interactions break the bipartite symmetry. In addition, the whole spectrum of the Hall conduction is obtained by the Kubo formula for the corresponding cases. The results are in accordance with the Thouless–Kohmoto–Nightingale–den Nijs integers when the Fermi energy lies in an energy gap. We find that the states due to the vacancies or impurities with small hopping constants are highly localized and do not contribute to the Hall conduction. However, the impurities with high hopping constants result in new Hall plateaus with constant conduction of $\sigma_{xy} = \pm e^2/h$, since high hopping constants increase the probability of an electron contributing to the conduction.

(Some figures may appear in colour only in the online journal)

1. Introduction

The problem of a particle moving in a periodic potential under the presence of a magnetic field has attracted attention since the early days of quantum mechanics. As was first shown by Hofstadter [1], the energy spectrum of this problem is a self-similar fractal structure when viewed as a function of the magnetic field. This self-similarity stems from the divisibility problem of the two length scales in the problem, the magnetic length and the lattice spacing. The integer quantum Hall effect for this system has also been studied and provides a disorder free model for Hall conductance quantization, as the Hall conductance for a system of fermions moving in such a periodic potential has been shown to be directly related to a topological invariant called the first Chern number [2].

Although this result of conductance quantization is theoretically well established, it remains experimentally unverified as of yet. The basic difficulty for electronic systems to get into the Hofstadter 'high magnetic field, strong lattice' limit is that experimentally unachievable magnetic fields of the order of thousands of Tesla are required to reduce the magnetic length to the order of the lattice spacing. However, recent developments in both solid state and cold atom physics show promise that this model can be experimentally realized. In solid state physics, it has recently been suggested that the presence of shear strain in graphene would act like an effective magnetic field for the electrons in certain limits [3]. In cold atom experiments the particles are neutral; however, a Berry phase that mimics an external magnetic field has been imprinted on the system using the coupling of internal states to suitably arranged lasers [4]. Using such a scheme very high artificial magnetic fields have been created and their physical effects such as vortices in a Bose condensate have been demonstrated [5]. Even more recently, very high staggered magnetic fields have been created in optical lattice potentials [6] and an experimental method for imprinting magnetic field induced phases on a lattice has been demonstrated [7]. These experiments provide a strong motivation for further theoretical consideration of this system.

We briefly review the theoretical progress on the response of a (2D) electronic system in a periodic potential to an applied magnetic field. There have been two different approaches to this problem. The first one is the semiclassical approach based on the Peierls and Onsager assumption [8, 9] which is applicable in the weak magnetic field limit. The second one is introduced for strong magnetic fields and assumes that the periodic lattice potential is a perturbation to the Landau level spectrum [10]. In 1964, Azbel [11] examined the behavior of Landau quantized electrons by considering the lattice potential as a perturbation term. Later, in 1976, Hofstadter [1] numerically studied the square tight-binding lattice under a magnetic field and obtained the fractal structure well known as the Hofstadter butterfly. After that, a similar problem for electrons in hexagonal lattices was studied [12]. The second order interactions with a square tight-binding lattice in a perpendicular magnetic field were introduced by Claro [13]. The symmetry properties of this problem were investigated by Zak and Brown [14, 15], by introducing the magnetic translation group which explains the splitting of the energy bands into the magnetic sub-bands from the perspective of group theory. Related problems such as the effect of magnetic modulation on Bloch electrons [16–18] or the Hofstadter butterflies for various lattices [19–24] have also been studied. Experimental data from (2D) antidot lattices provide indirect evidence for the existence of the Hofstadter butterfly [25], along with the theoretical investigations for this system [26, 27].

One of the most important properties of lattice electrons under a magnetic field is that they provide a disorder free model for Hall conductance quantization, i.e. the integer quantum Hall effect. When the Fermi level is in an energy gap, the value of the Hall conduction is expressed in terms of the famous Thouless–Kohmoto–Nightingale–den Nijs (TKNN) integers [2, 28] times e^2/h. The whole picture for the conductance can be calculated either by the Streda [29] formula originating from the linear response theory or by the Kubo formalism. Several works have been published which have concentrated on both the Hall conduction and the Hofstadter butterflies for the cases of square, triangular, kagomé and honeycomb lattices [30–40].

However, the effects of imperfectness of the lattice on the electronic structure, such as the presence of point defects, have not been fully studied. In this work, we investigate the spectrum (Hofstadter butterfly) and the Hall conductance of the system when impurities are introduced into the lattice. Such impurities would be naturally present in a solid state system, and can be easily introduced into an optical lattice cold atom system by redesigning the optical lattice or by including a mixture of other atomic species as in recent experiments [41–43]. We not only consider the nearest neighbor hopping but also include the next nearest neighbor hopping within the tight-binding methodology. By including the next nearest neighbor interactions, we make sure that our results for impurities are robust with respect to the breaking of the bipartite symmetry of the lattice. In this work, we consider a square lattice which is commonly used in cold atom experiments, but our methods are equally applicable to other lattice geometries.

We explore the evolution of the Hofstadter butterfly and the Hall conductance with the imperfections. Our results show that the presence of an impurity in general shifts the Hofstadter bands. Depending on the impurity concentration and strength certain bands of the spectrum may merge, altering the value of the Hall conductance. The contribution of the impurity state to the Hall conductance decreases when the impurity state is more localized, as expected. We also present a method for efficiently forming the tight-binding matrix for supercells in this model. The paper is organized as follows. In section 2, we review the pure lattice spectrum and discuss how impurities can be introduced by expanding the unit cell. We show how the tight-binding matrix for the enlarged unit cell can be efficiently constructed. In section 3, we present the energy spectra and the Hall conductances in the presence of point defects and systematically analyze the results as a function of impurity strength. Finally, in section 4, we conclude by pointing out the key results and briefly discussing how can they be experimentally accessed.

2. Methodology

We use the tight-binding method for the square lattice where the first and second nearest neighbor interactions are both included in order to model the (2D) electronic system in a magnetic field, with impurities or vacancies. The perpendicular magnetic field applied to the (2D) system brings out additional phase factors [8] to the usual tight-binding terms. In addition, the magnetic field changes the periodicity of the system leading to a larger ‘magnetic unit cell’. Once the tight-binding system is revised with the magnetic field, we end up with a new magnetic field tight-binding Hamiltonian, which is described by the A_m matrix [1]. Its eigenvalues and eigenvectors give the desired energies and wavefunctions, respectively.

For a pure system, a square lattice with a single atom basis works well, and it has produced many results about the Hofstadter butterflies and the Hall conductances [44–46]. There are also studies [47] on the effect of second nearest neighbor interactions which break the bipartite symmetry. When the system has only the first order interactions, each site can be considered as a composition of two sublattices. For such a system there is only inter-sublattice hopping. If there is an eigenfunction with energy E, changing the sign of this eigenfunction on one sublattice yields another eigenfunction with energy $-E$. As a result of that, the eigenvalues come out in pairs $(E, -E)$ and the energy spectrum is symmetric around the $E = 0$ line. However, second nearest neighbor interactions introduce intra-layer hopping which breaks the bipartite symmetry. Therefore, in the presence of intra-layer hopping the Hofstadter butterfly is no longer symmetric around $E = 0$.

For the impurity and vacancy cases the tight-binding method with a single atom in the basis is not enough to realistically model the case. One has to have at least two atoms in order to treat one of them as an impurity or vacancy. However, for this scenario, we get 50% of impurity or vacancy in terms of concentration which is similar to a superlattice

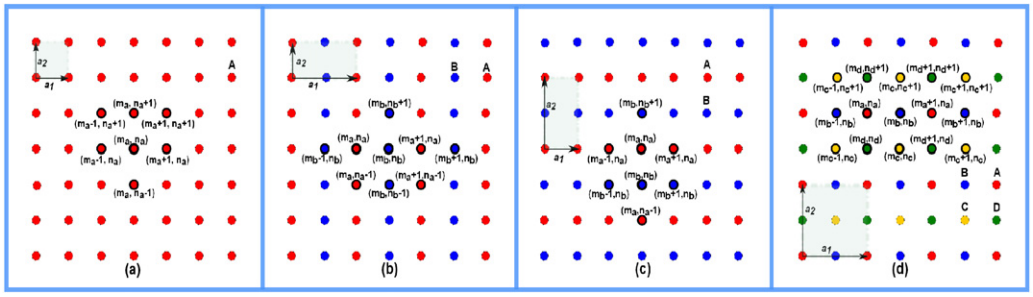

Figure 1. The unit cells for the configurations. (a) One atom in the basis. The corresponding lattice vectors are $\vec{a}_1 = \hat{x}a$ and $\vec{a}_2 = \hat{y}a$, where $a = 1$ is the lattice constant. (b) Rectangular unit cell aligned horizontally: two atoms in the basis with an asymmetric choice of unit cell. The corresponding lattice vectors are $\vec{a}_1 = 2a\hat{x}$ and $\vec{a}_2 = a\hat{y}$. (c) Rectangular unit cell aligned vertically: asymmetric unit cell choice of a square lattice which contains again two atoms but with different unit vectors. The corresponding lattice vectors are $\vec{a}_1 = \hat{x}a$ and $\vec{a}_2 = \hat{y}2a$. (d) Square lattice which contains four different atoms in the unit cell. The lattice vectors are $\vec{a}_1 = \hat{x}2a$ and $\vec{a}_2 = \hat{y}2a$.

rather than an impurity. In order to overcome this obstacle, one should choose the unit cell as large as possible. In this paper, we are proposing a method which enables direct access to the A_m matrix. This matrix is obtained by the tight-binding method under the perpendicular magnetic field, which can be written in the form of the well-known Harper's equation [49]. We show how to generate the A_m matrix efficiently for enlarged supercells of the square lattice. In order to establish the method for enlarged systems which include a point defect with reasonable density, we present the cases starting from a small single atom unit cell to an enlarged unit cell including nine atoms. Although we are discussing the specific case for the square lattice, our methods are applicable to all kinds of lattice geometries.

2.1. Square lattice with a single atom in the basis

We start by reviewing the pure case which was first discussed by Hofstadter [1]. Within the tight-binding approximation, the single band Hamiltonian for the Schrödinger equation of a square lattice with lattice constant a, for one atom in the unit cell is equal to

$$H = t\{e^{-ik_x a} + e^{ik_x a} + e^{-ik_y a} + e^{ik_y a}\}, \tag{1}$$

where the exponential factors arise due to the interactions of the first nearest neighbors. The coefficient t is the hopping (orbital interaction) term which has units of energy. Henceforth, we will express all energies in units of t, effectively setting $t = 1$. The geometric configuration can be viewed from figure 1(a) where one can observe that the atom with label (m_a, n_a) interacts with the atoms of labels $(m_a + 1, n_a)$, $(m_a - 1, n_a)$, $(m_a, n_a + 1)$, and $(m_a, n_a - 1)$. The corresponding lattice vectors $\vec{a}_1$ and $\vec{a}_2$ satisfy the equation $\vec{R}_{(m_a,n_a)} = m_a\vec{a}_1 + n_a\vec{a}_2$, where $\vec{R}_{(m_a,n_a)}$ is the position vector of the atom labeled by (m_a, n_a). When we introduce the magnetic field into the system, we use the Peierls substitution which shifts the momentum with the vector potential of the magnetic field,

$$\hbar\mathbf{k} \to \hbar\mathbf{k} - \frac{e\vec{\mathbf{A}}}{c}.$$

For a perpendicular magnetic field, we choose the Landau gauge which gives a vector potential in the y direction as a function of x, $\vec{\mathbf{A}} = (0, Bx, 0)$. With this choice of gauge, only the hopping strengths in the y direction gather additional phase factors $e^{-2\pi i \frac{e}{\hbar}\int \vec{\mathbf{A}}\cdot\vec{dl}}$, where the integral is evaluated along the line connecting the two atoms. With the addition of the magnetic field originated phase factors, we have a new Hamiltonian

$$H' = t\{e^{-ik_x a} + e^{ik_x a} + e^{-ik_y a}e^{2i\pi m_a \frac{\phi}{\phi_0}} + e^{ik_y a}e^{-2i\pi m_a \frac{\phi}{\phi_0}}\},$$

where $\phi = Ba^2$, the magnetic field times the area of the unit cell, and ϕ_0 is the flux quanta h/e. Now, the Schrödinger equation becomes

$$\begin{aligned} H'\psi &= t\psi(m_a - 1, n_a) + \psi(m_a + 1, n_a) \\ &\quad + \psi(m_a, n_a - 1)e^{2i\pi m_a \frac{\phi}{\phi_0}} \\ &\quad + \psi(m_a, n_a + 1)e^{-2i\pi m_a \frac{\phi}{\phi_0}} \\ &= \varepsilon\psi(m_a, n_a). \end{aligned}$$

If we make the substitution $\psi(m_a, n_a) = \varphi(m_a)e^{ik_y a n_a}$, we get a new equation known as Harper's equation,

$$\begin{aligned} \varepsilon\varphi(m_a) &= t\varphi(m_a - 1) + t\varphi(m_a + 1) \\ &\quad + 2t\varphi(m_a)\cos\left(2\pi m_a \frac{\phi}{\phi_0} - k_y a\right). \end{aligned} \tag{2}$$

We set the ratio between the amount of flux through a plaquette and the flux quantum to be equal to α, and let this α be represented as a fraction of two co-prime integers such that $\alpha = \phi/\phi_0 = p/q$. The value of m_a ranges from 1 to q. However, when we try to solve this recursive equation for $\varphi(1)$, we have a $\varphi(0)$ term on the right-hand side. Similarly, when we set m_a to be $m_a = q$, we have a $\varphi(q + 1)$ term on the right-hand side. In order to obtain solutions to this equation, we have to stay within the boundaries we decided for m_a which spans the values from 1 to q. For this purpose, we apply the Bloch condition which can be expressed as $\varphi(m + q) = \varphi(m)e^{iqk_x a}$. By use of this boundary condition, we end up with a matrix equation. This supercell matrix is

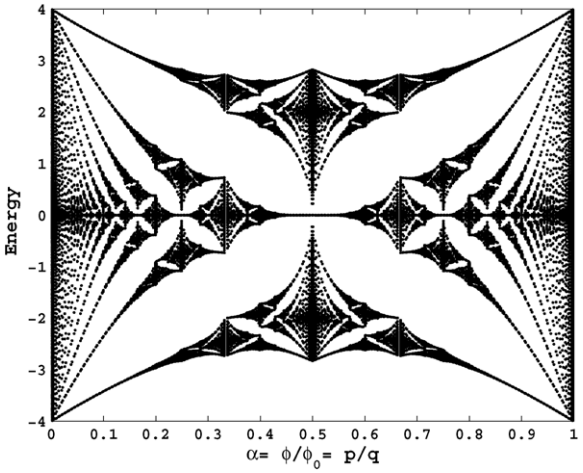

Figure 2. The Hofstadter butterfly spectrum for a square lattice with $q = 501$ and $t = 1.0$.

called the A_m matrix,

$$\begin{bmatrix} \varphi_1 \\ \varphi_2 \\ \vdots \\ \varphi_{q-1} \\ \varphi_q \end{bmatrix} = \begin{bmatrix} 2t\cos\left(2\pi\frac{\phi}{\phi_0}\right) & t & 0 & \cdots & te^{-iqk_xa} \\ t & 2t\cos\left(4\pi\frac{\phi}{\phi_0}\right) & t & \cdots & 0 \\ 0 & t & 2t\cos\left(6\pi\frac{\phi}{\phi_0}\right) & t & \vdots \\ \vdots & \vdots & \ddots & \ddots & t \\ te^{iqk_xa} & 0 & \cdots & t & 2t\cos\left(2q\pi\frac{\phi}{\phi_0}\right) \end{bmatrix} \times \begin{bmatrix} \varphi_1 \\ \varphi_2 \\ \vdots \\ \varphi_{q-1} \\ \varphi_q \end{bmatrix}, \quad (3)$$

and the eigenvalues of this matrix have the famous butterfly shape given in figure 2. In order to model enlarged systems we propose a method through which we construct the A_m matrix just by the help of the geometric configurations. We first show how to enlarge the unit cell of a pure system, and then generalize this method to model point defects.

2.2. Enlarged unit cell

Assume that we have a square lattice with two atoms in its basis, labeled by **A** and **B**, that are arranged as shown in figure 1(b). For this case, differently from equation (1), we have the matrix representation for the Hamiltonian

$$H = \begin{bmatrix} H^{AA} & H^{AB} \\ H^{BA} & H^{BB} \end{bmatrix}.$$

These independent matrices have the information for the orbital interactions between the types of atom located at the nearest neighboring sites. For example, H^{AA} has three terms: the self-interaction term of the type A atom plus two terms for the interaction of neighboring type A atoms. Due to the addition of the magnetic field, there will be phase factors for only those interactions which are aligned with the vector potential in the y direction. We can expand the Hamiltonian with the phase factors arising from the magnetic field under these circumstances,

$$H^{AA} = t\{e^{ik_ya}e^{-i\theta} + e^{-ik_ya}e^{i\theta}\} + \varepsilon_{2p},$$
$$H^{AB} = t\{e^{ik_xa} + e^{-ik_xa}\},$$

where ε_{2p} is the self-interaction term of p_z orbitals. Since the Hamiltonian must be a Hermitian matrix, H^{BA} is the complex conjugate of H^{AB}. The extra exponential terms in H^{AA} can be defined as follows:

$$e^{i\theta} = e^{-2\pi i\int_{R_{m_a,n_a-1}}^{R_{m_a,n_a}}\vec{A}\cdot d\vec{l}}, \quad = e^{2\pi i(2a^2Bm_a)\frac{e}{\hbar}} = e^{2\pi i\frac{\phi}{\phi_0}m_a}.$$

Due to the change in the area of the unit cell, we now have $\phi = 2Ba^2$, which is doubled compared to the square lattice with one atom in its unit cell. Another difference from the previous calculation is that we have a column vector for the $\varphi(m_a)$ which we choose to denote as

$$\Psi(m) = \begin{bmatrix} \varphi(m_a) \\ \varphi(m_b) \end{bmatrix}.$$

According to these considerations, equation (2) is now a matrix equation,

$$\Psi(m) = U_m\Psi(m) + W_m\Psi(m-1) + V_m\Psi(m+1), \quad (4)$$

where U_m, W_m, and V_m are all matrices, instead of single coefficients as in the pure case. Explicitly,

$$U_m = \begin{bmatrix} 2t\cos(2\pi\alpha m - k_ya) & t \\ t & 2t\cos(2\pi\alpha(m+1/2) - k_ya) \end{bmatrix},$$
$$W_m = \begin{bmatrix} 0 & t \\ 0 & 0 \end{bmatrix}, \qquad V_m = \begin{bmatrix} 0 & 0 \\ t & 0 \end{bmatrix}.$$

We apply the Bloch condition to the wavefunctions and, as a result, we have the A_m matrix as follows:

$$A_m = \begin{bmatrix} U_1 & V_1 & 0 & 0 & \cdots & 0 & W_1^* \\ W_2 & U_2 & V_2 & 0 & 0 & \cdots & 0 \\ 0 & W_3 & U_3 & V_3 & 0 & \cdots & 0 \\ \vdots & \vdots & \ddots & \ddots & \ddots & \ddots & \vdots \\ V_q^* & 0 & 0 & \cdots & 0 & W_q & U_q \end{bmatrix}. \quad (5)$$

2.2.1. Rectangular unit cell aligned horizontally. For a system of atoms arranged as in figure 1(b), it is somehow easy to perform this calculation; however, we are offering a simple and compact method in order to construct the A_m matrix just from the geometry. Therefore, it is sufficient to calculate

the phase factors due to the perpendicular magnetic field on top of the simple tight-binding methodology. As pointed out previously, only the hopping in the y-direction is modified by the magnetic field. Since we have two types of atom in the unit cell, and the periodicity of the phase factors in the m direction is q, the dimensions of the A_m matrix are $2q \times 2q$. We start by generating the A_m matrix as a $2q \times 2q$ null matrix. The first element (1, 1) of the matrix A_m will be due to the interaction of the A atom labeled by ($m_a = 1$) with the A atoms with the same label ($m_a = 1$). As there are two A type atoms with labels ($m_a = 1$) in the first nearest neighborhood there is a term $2t\cos(2\pi\frac{\phi}{\phi_0} - k_y a)$ in the $A_m(1, 1)$. Our next term will be $A_m(1, 2)$, which has the value t due to the interaction between atom type A labeled by ($m_a = 1$) and atom type B labeled by ($m_b = 1$). The matrix element A_m with index (1, 3) is equal to 0, since we do not consider such a long range interaction. Similarly, $A_m(1, 4)$ is equal to 0, as well as the rest of this row. In order to include the second nearest neighbors or even higher order hopping, we would have to calculate longer range tight-binding terms. In the next row, the same procedure is repeated but for this case we are concentrating on the interactions between the atom B($m_b = 1$) and A($m_a = 1$), B($m_b = 1$), A($m_a + 1$) = A(2), B($m_b + 1$) = B(2). So we have

$$A_m(2, 1) = t,$$
$$A_m(2, 2) = 2t\cos\left(2\pi\frac{\phi}{\phi_0}(1 + 1/2) - k_y a\right),$$
$$A_m(2, 3) = t, \qquad A_m(2, 4) = 0.$$

Again this row spans all the values in the range $m = 1, 2, \ldots, q$. The rest of the rows can be calculated by carrying out the same steps from m_a to $m_a + q$, and we end up with

$$A_m = \begin{bmatrix} 2t\cos\left(2\pi\frac{\phi}{\phi_0} - k_y a\right) & t & 0 & \cdots & 0 \\ t & 2t\cos\left(2\pi\frac{\phi}{\phi_0}(1 + 1/2) - k_y a\right) & t & & 0 \\ 0 & t & 2t\cos\left(4\pi\frac{\phi}{\phi_0} - k_y a\right) & & 0 \\ \vdots & \vdots & & \ddots & \vdots \\ 0 & 0 & 0 & \cdots & 0 \\ 0 & 0 & \cdots & 0 & \\ 0 & 0 & \cdots & 0 & \\ t & 0 & \cdots & 0 & \\ \ddots & \ddots & \ddots & \vdots & \\ \cdots & 0 & t & 2t\cos\left(2\pi\frac{\phi}{\phi_0}(q + 1/2) - k_y a\right) & \end{bmatrix}. \quad (6)$$

Now we have to apply the Bloch condition to the wavefunctions $\psi(m_a + q - 1) = e^{ik_x qa}\psi(m_a - 1)$, through which we determine the topmost right-hand side and the bottommost left-hand side of the matrix A_m. Let us start with the bottommost entries $A_m(2q - 1, 1)$, $A_m(2q - 1, 2)$, $A_m(2q, 1)$ and $A_m(2q, 2)$, which represent the interactions of A($m_a + q - 1$) with A(m_a) and B(m_b), and B($m_b + q - 1$) with A(m_a) and B(m_b), since we have to have q elements in each row and column. Thus,

$$A_m(2q - 1, 1) = 0 \cdot e^{ik_x qa}, \qquad A_m(2q - 1, 2) = 0 \cdot e^{ik_x qa},$$
$$A_m(2q, 1) = te^{ik_x qa}, \qquad A_m(2q, 2) = 0 \cdot e^{ik_x qa}.$$

The eigenvalues of the A_m give the energy as a function of flux which is a real physical observable, so A_m is Hermitian,

Table 1. The scheme for the interactions between the atoms.

Atom label	First N N interactions	Second NN interactions
Atom A	B, D	C
Atom B	A, C	D
Atom C	B, D	A
Atom D	A, C	B

i.e. $A_m(i, j) = A_m^*(j, i)$, and we obtain the resulting A_m:

$$A_m = \begin{bmatrix} 2t\cos\left(2\pi\frac{\phi}{\phi_0} - k_y a\right) & t & 0 & \cdots & te^{-ik_x qa} \\ t & 2t\cos\left(2\pi\frac{\phi}{\phi_0}(1 + 1/2) - k_y a\right) & t & & 0 \\ 0 & t & 2t\cos\left(4\pi\frac{\phi}{\phi_0} - k_y a\right) & & 0 \\ \vdots & \vdots & & \ddots & \vdots \\ te^{ik_x qa} & 0 & 0 & \cdots & 0 \\ 0 & 0 & \cdots & te^{-ik_x qa} & \\ 0 & 0 & \cdots & 0 & \\ t & 0 & \cdots & 0 & \\ \ddots & \ddots & \ddots & \vdots & \\ \cdots & 0 & t & 2t\cos\left(2\pi\frac{\phi}{\phi_0}(q + 1/2) - k_y a\right) & \end{bmatrix}. \quad (7)$$

This scheme for the generation of the A_m matrix can be viewed via figure 3, which is suitable for our case of an enlarged unit cell aligned horizontally. The rows and the columns are reserved for the atoms of the corresponding labels. The entries of the A_m matrix correspond to the interactions of the atoms denoted by the labels and indices of the interacting atoms.

2.2.2. Rectangular unit cell aligned vertically. If we have a similar geometric alignment to that seen in figure 1(c), we can easily generate the A_m matrix by following the same steps as we did for figure 1(b). The only things we should know additionally are the phase factors. We have $te^{\pi\frac{\phi}{\phi_0} - k_y a}$ terms in addition to the tight-binding terms between the atom A(m_a) and atoms B(m_b), and also between the atom B(m_b) and atoms A(m_a). Differently from the previous example, here we have a $4q \times 4q$ A_m matrix because of the periodicity of the exponential factor with $2q$, and we have two different types of atom,

$$A_m = \begin{bmatrix} 0 & 2t\cos\left(\pi\frac{\phi}{\phi_0} - k_y a\right) & t & 0 & \cdots & te^{-ik_x 2qa} & 0 \\ 2t\cos\left(\pi\frac{\phi}{\phi_0} - k_y a\right) & 0 & 0 & t & 0 & \cdots & te^{-ik_x 2qa} \\ t & 0 & 0 & 0 & \cdots & 0 & \\ 0 & t & 2t\cos\left(2\pi\frac{\phi}{\phi_0} - k_y a\right) & 0 & \cdots & 0 & \\ te^{ik_x 2qa} & \vdots & \ddots & 0 & \cdots & 0 & \\ 0 & te^{ik_x 2qa} & 0 & \ddots & \ddots & \vdots & \\ 0 & 0 & \cdots & \cdots & t & 2t\cos\left(4q\pi\frac{\phi}{\phi_0} - k_y a\right) & 0 \end{bmatrix}. \quad (8)$$

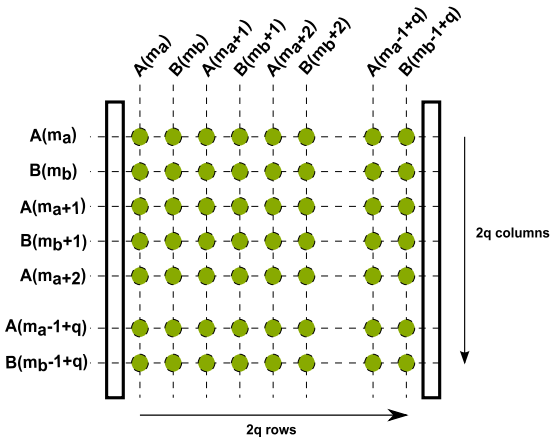

Figure 3. The organization scheme for the A_m matrix shown for two kinds of atom in the unit cell.

2.2.3. A more general example: a square lattice of four atoms in the unit cell with second nearest neighbor interactions. Now, suppose that we have a square lattice in which we have four different atoms oriented as shown in figure 1(d). For this case, since we have four different atoms, we have the wave vectors as

$$\Psi(m) = \begin{bmatrix} \varphi(m_a) \\ \varphi(m_b) \\ \varphi(m_c) \\ \varphi(m_d) \end{bmatrix},$$

and we also have a 4×4 block Hamiltonian

$$H = \begin{bmatrix} H^{AA} & H^{AB} & H^{AC} & H^{AD} \\ H^{BA} & H^{BB} & H^{BC} & H^{BD} \\ H^{CA} & H^{CB} & H^{CC} & H^{CD} \\ H^{DA} & H^{DB} & H^{DC} & H^{DD} \end{bmatrix}.$$

If we consider both the first and the second nearest neighbor interactions, we have the interaction scheme shown in table 1. For example, atom A will have first order interactions with two atoms labeled by B and two atoms labeled by D, and also it will have second order interactions with four atoms all labeled by C. We have the phase factors due to the magnetic field through the interactions which align in the y direction as well as the ones which have a non-zero y direction component. As result, speaking in terms of the atom A(m_a), we will have $2\cos(\pi\frac{\phi}{\phi_0}m_a - k_y a) = \theta(\mathrm{AD}_1)$ for the interaction with D atoms, $2\cos(\pi\frac{\phi}{\phi_0}(m_a - 1/4) - k_y a) = \theta(\mathrm{AC}_2)$ for the interaction with the atoms labeled by C($m_c - 1$) and $2\cos(\pi\frac{\phi}{\phi_0}(m_a + 1/4) - k_y a) = \theta(\mathrm{AC}_1)$ due to the interaction with the atoms labeled by C(m_c). In addition, let us denote the second order tight-binding interaction coefficient as t'. After incorporating the Bloch condition, and calculating the magnetic phase factors for the rest of the atoms, we can write the A_m matrix

$$A_m = \begin{bmatrix} 0 & t & t'\theta(\mathrm{AC}_1) & t\theta(\mathrm{AD}_1) & 0 & \cdots & 0 & te^{-ik_x 2qa} & t'\theta(\mathrm{AC}_2)e^{-ik_x 2qa} \\ t & 0 & t\theta(\mathrm{BC}_1) & t'\theta(\mathrm{BD}_1) & t & \cdots & 0 & t'\theta(\mathrm{BD}_2) & 0 \\ \vdots & \vdots & \vdots & \vdots & \vdots & \cdots & \vdots & 0 & \vdots \\ 0 & 0 & 0 & 0 & 0 & \cdots & 0 & \cdots & \vdots \\ t'\theta(\mathrm{CA}_1)e^{ik_x 2qa} & 0 & 0 & te^{ik_x 2qa} & 0 & \cdots & \vdots & \ddots & \vdots \\ 0 & 0 & 0 & 0 & \cdots & \cdots & t'\theta(\mathrm{BD}_2) & t\theta(\mathrm{DA1}) & t'\theta(\mathrm{DB1}) \\ & & & & & & t & 0 & \end{bmatrix}. \quad (9)$$

2.3. Square lattice with nine atoms in the basis

With the scheme outlined above, we can expand our unit cell as needed. We use an enlarged unit cell composed of nine atoms to model impurities or vacancies, corresponding to a point defect concentration of $1/9 \simeq 11\%$. We label the atoms with the letters 'A, B, ..., E, ..., H, I'. We pick the fifth one with label 'E' and treat it as a vacancy or impurity by modifying its hopping constants. We leave the remaining atoms with the usual square lattice first order hopping constant $t = 1.0$, and the second order hopping constant is set to 0.05 which is almost of the same order as the second nearest neighbor calculations made by Hatsugai and Kohmoto [47].

Similarly to the density functional theory which is also used to model doped systems or systems with imperfections, we use a periodic unit cell to model the system [48]. As a result of that, any change in the unit cell repeats itself periodically. In real condensed matter samples the distribution of impurities is random. The model we use is not realistic in that sense, in that the imperfections are regularly distributed. However, as long as the states localized at the imperfections are confined to a region which is smaller than our enlarged unit cell, our method should be sufficient to describe their effects. Moreover, for the cold atom experiments, it is possible to design arbitrary lattices. From this paper, it is not unrealistic to have a square lattice with periodic imperfections. The position of the impurity atom in the enlarged unit cell does not cause any changes since the system is infinite and the enlarged unit cell repeats itself periodically through all directions.

Due to the change in the magnetic phase factors, our system is now $3q$ periodic, and since we have nine atoms in the basis, the resulting A_m matrix has the dimension of $27q \times 27q$. The magnetic unit cell for the corresponding case is given in figure 4. The magnetic unit cell is the combination of enlarged unit cells arranged horizontally due to the chosen Landau gauge, i.e. $\vec{\mathbf{A}} = (0, Bx, 0)$. In the magnetic unit cell each of nine atoms defined by labels 'A, B, ..., E, ..., H, I' inside the enlarged unit cell is connected to $3q$ atoms. The first enlarged unit cell atoms have the labels 'A1, B1, ..., E1, ..., H1, I1' while the last enlarged unit cell atoms are labeled by 'A3q, B3q, ..., E3q, ..., H3q, I3q'. Due to periodicity, the

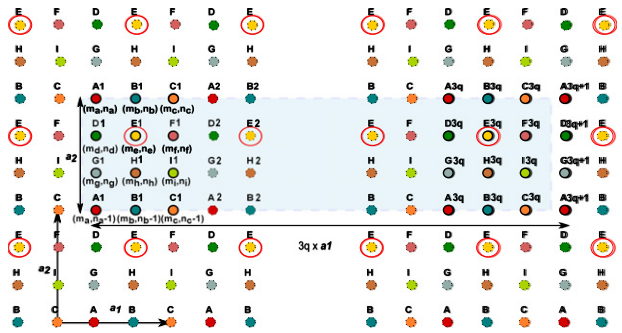

Figure 4. The magnetic unit cell of the square lattice with nine atoms in the basis of the unit cell and $27q$ atoms in the basis of the magnetic unit cell. The encircled atoms with label 'E' are treated as impurities or vacancies.

last atoms labeled with $3q + 1$ are identical with the ones in the first enlarged unit cell, apart from a certain phase factor which is the Bloch condition. With a procedure similar to that performed in section 2.2.3, we easily generate the A_m matrix, with or without the next nearest neighbor hopping. We alter the hopping constant of the interactions involving the atom labeled 'E' in the A_m matrix. The eigenvalues of the A_m matrix for all the k-points in the magnetic Brillouin zone as a function of $\alpha = \phi/\phi_0$ give the Hofstadter butterfly in the presence of the point defects.

3. Results and discussion

3.1. Electronic spectrum: Hofstadter butterfly

We follow the procedure that we described in section 2.2 for the modeling of an impurity or a vacancy located on a lattice point (substitutional position) of the square lattice. The unit cell as well as the magnetic unit cell can be viewed in figure 4. In this figure, an atom treated as an impurity or a vacancy is labeled with 'E'. As a first step, we consider only the first nearest neighbor interactions. We call the nearest neighbor hopping constant for atom 'E' t_{E}, again measured in units of t. We alter this parameter t_{E} in the range from 1.5 to 0.001 for the impurity cases, while we obtain the vacancy case for $t_{\mathrm{E}} = 0$. Note that we get the pure case when $t_{\mathrm{E}} = 1.0$, corresponding to the case where all the atoms are the same. The impurity or the vacancy case replacing one atom out of nine atoms corresponds to a defect concentration of the order of 11%.

After diagonalizing the A_m matrix we get the energy eigenvalues as a function of $\alpha = \phi/\phi_0$. The Hofstadter butterflies for selected values of the parameter t_{E} are plotted in figure 5. The range of α defined as the flux per enlarged unit cell is set from 0 to 18, in accordance with the results where we include the second order interactions. As displayed in figure 6 for the latter case, there is an extra envelope like periodicity within the butterflies. The pure case with $t_{\mathrm{E}} = 1.0$ labeled by (f) is the same spectrum as that plotted for a single atom in figure 2. The only difference between these two plots is the periodicity in α because α in our notation is the magnetic flux per enlarged unit cell. In both of the spectra, there is a zero energy band which divides up the graph horizontally into two identical parts. This is a consequence of the bipartite symmetry of the square lattice. When we set $t_{\mathrm{E}} = 0.75$, we see a different spectrum with new gaps and bands formed as shown in figure 5(d). For the case where we reduce t_{E} to 0.50, we see the emergence of dome shaped gaps around $\alpha = 4.5$ and 13.5 with energy values of ± 0.8 as plotted in figure 5(c). Within these gaps, the Hall conductance is zero as discussed in section 3.2. A sequence of bands are formed between the dome shaped gaps which are symmetric about $E = 0$. These bands are clearly related to states localized around the impurity. As we continue to reduce t_{E}, i.e. $t_{\mathrm{E}} = 0.25$ shown in figure 5(b), we see that these gaps become more elliptic compared to figure 5(c). We also note that the 'impurity bands' between the domes approach the horizontal energy line $E = 0$. One limit of the impurity case is the vacancy, where $t_{\mathrm{E}} = 0$, and its spectrum displayed in figure 5(a) shows elliptic gaps around $E = 0$. Moreover, the 'impurity bands' now collapse to the $E = 0$ line, signifying that the impurity is decoupled from the rest of the system. In the opposite limit we also consider the impurity with a stronger hopping constant. We examine this situation for $t_{\mathrm{E}} = 1.50$ and display the corresponding Hofstadter butterfly in figure 5(f). For this strongly coupled impurity, the spectrum is modified near the maximum and minimum energy values. Hence, the bands due to the impurity states appear near $E = \pm 4$ as clearly seen in figure 5(f). The low energy structure ($E \sim 0$) remains mostly unmodified by the presence of the strongly coupled impurity.

The effect of the second nearest neighbor interactions on the Hofstadter butterfly was thoroughly examined in [47]. Inclusion of the next nearest neighbor interactions is important for two reasons. First they would be present in a solid state system and also in a cold atom system as long as the optical lattice is not too deep. Second, even if they are weak, such interactions break the bipartite symmetry of the lattice. As a result the spectrum is no longer symmetric about $E = 0$. Thus, by including the next nearest neighbor interactions, we make sure that the results for our impurities are robust with respect to the breaking of the bipartite symmetry. As we introduce second order hoppings, the butterfly loses its mirror symmetry around the $\alpha = 4.5$ and 13.5 lines. The gaps and bands gain positive (negative) shifts for $\alpha > 4.5$ ($\alpha < 4.5$). This shift is reversed near the $\alpha = 13.5$ line. As a result of the self-similar structure of the butterfly, similar shifts appear at other principal rational fractions with even denominators. In addition to this, the spectrum gains a new envelope like periodicity. In order to display this new periodicity, we plotted our butterflies as a function of α from 0 to 18. The corresponding spectra for different impurity cases are presented in figure 6. While the widths of gaps and bands change, there is no qualitative difference in the number and location of the gaps when compared to figure 5. Most importantly, the dome shaped gaps and impurity bands observed with only first order interactions are robust with respect to second order hopping. These structures are shifted in accordance with the general spectrum, nonetheless their general properties remain unaltered.

The impurity states result in new gaps and bands in the Hofstadter butterfly. In the energy spectra they are responsible

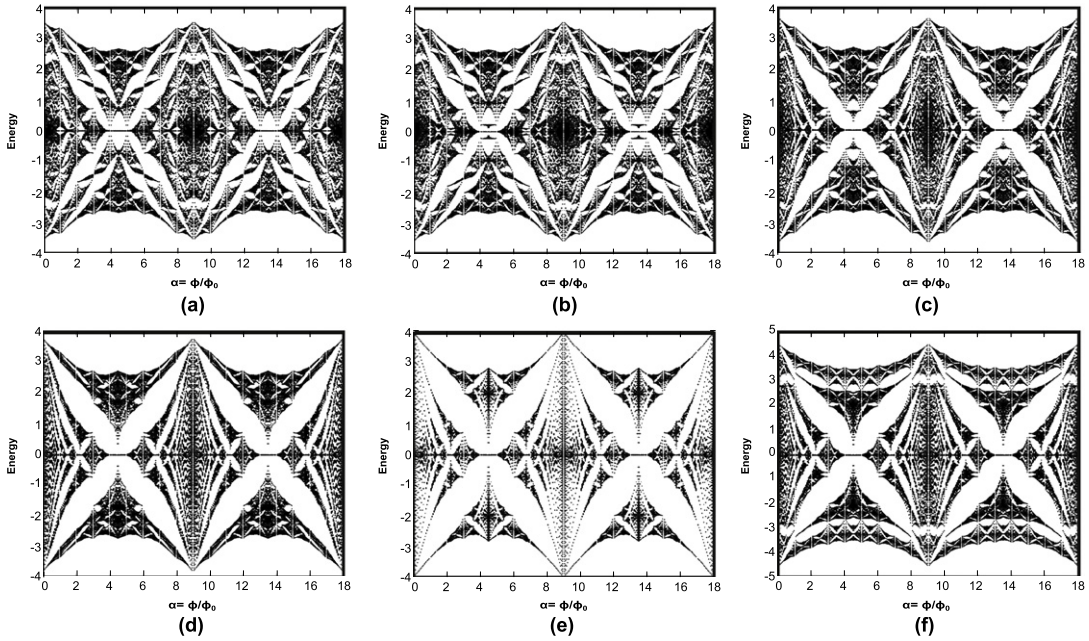

Figure 5. Energy (in units of 't') versus $\alpha = p/q = \phi/\phi_0$ defined as the flux per enlarged unit cell, results in the Hofstadter butterflies for the following cases: (a) 'E' is a vacancy with $t_{\mathrm{E}} = 0.0$; (b) 'E' is an impurity with $t_{\mathrm{E}} = 0.25$; (c) 'E' is an impurity with $t_{\mathrm{E}} = 0.50$; (d) 'E' is an impurity with $t_{\mathrm{E}} = 0.75$; (e) all of the atoms are the same with $t_{\mathrm{E}} = 1.00$; (f) 'E' is an impurity with $t_{\mathrm{E}} = 1.50$.

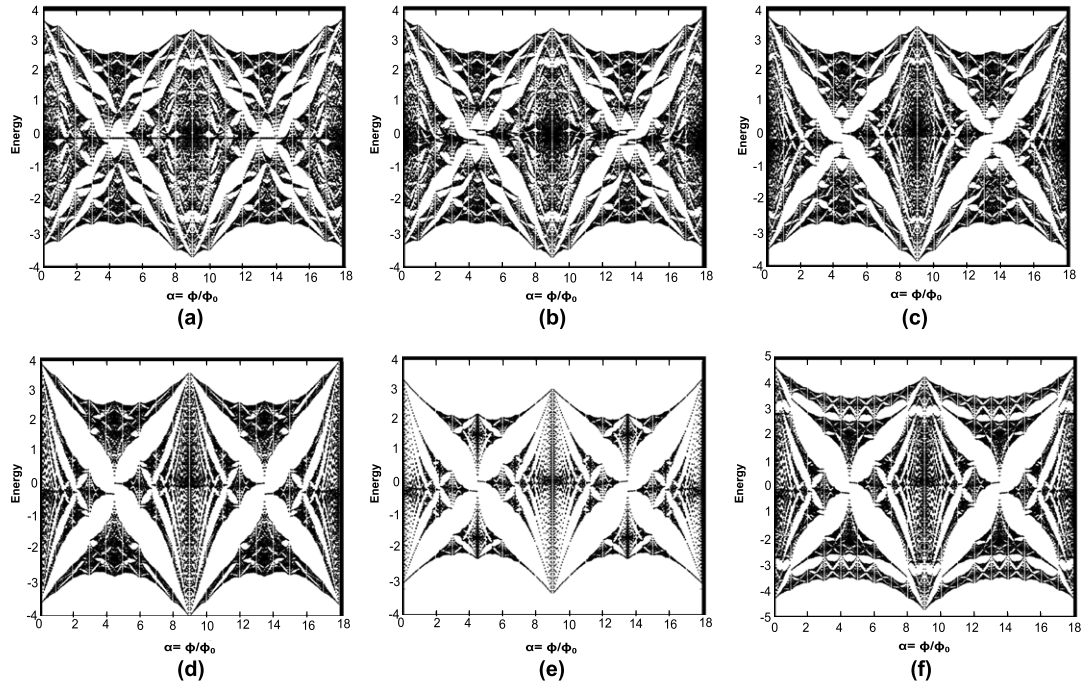

Figure 6. Energy (in units of 't') versus $\alpha = p/q = \phi/\phi_0$ defined as the flux per enlarged unit cell, results in the Hofstadter butterflies. Both the first and the second nearest neighbor interactions are considered, for the following impurity and vacancy cases: (a) 'E' is a vacancy with $t_{\mathrm{E}} = 0.0$ and $tt_{\mathrm{E}} = 0.0$; (b) 'E' is an impurity with $t_{\mathrm{E}} = 0.25$ and $tt_{\mathrm{E}} = 0.025$; (c) 'E' is an impurity with $t_{\mathrm{E}} = 0.50$ and $tt_{\mathrm{E}} = 0.025$; (d) 'E' is an impurity with $t_{\mathrm{E}} = 0.75$ and $tt_{\mathrm{E}} = 0.025$; (e) all of the atoms are the same with $t_{\mathrm{E}} = t = 1.00$ and $tt_{\mathrm{E}} = tt = 0.05$; (f) 'E' is an impurity with $t_{\mathrm{E}} = 1.50$ and $tt_{\mathrm{E}} = 0.075$.

for new self-similar structures near the $E = 0$ line or at the extrema regions of the spectra depending on their hopping strength. This self-similar structure with such well defined gaps and bands is due to the periodic arrangement of the imperfections. This periodicity originates from the limitations of our tight-binding method. However, in a real sample in which the imperfections are distributed within the system randomly, the regions in the Hofstadter butterfly modified by these states will still exist. We believe that they will lose their self-similar structure, and the gaps will be blurred

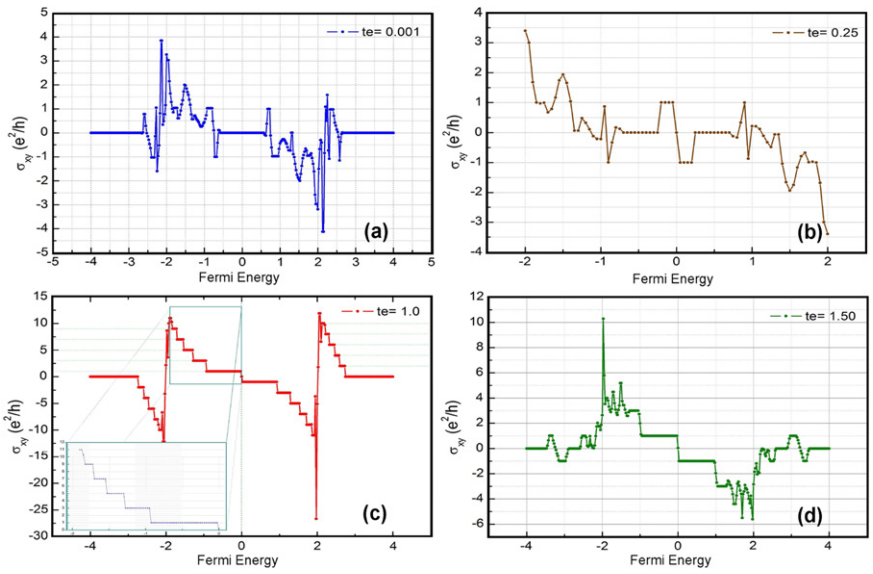

Figure 7. Hall conductivities (in units of e^2/h) as a function of the Fermi energy (in units of 't') with the first order interactions where α is set to $p/q = 13/3$: (a) 'E' is an impurity with $t_E = 0.001$; (b) 'E' is an impurity with $t_E = 0.25$; (c) all of the atoms are the same with $t_E = t = 1.00$; the inset shows a zoom in of the region of the spectrum enclosed by a rectangle; (d) 'E' is an impurity with $t_E = 1.50$.

due to the random arrangement. The scaling theory of conduction of course predicts that randomness causes all states to be localized in two dimensions due to Anderson localization [50]. However, in usual cold atom experiments the predicted localization length is much larger than the system size. Thus, our method remains a good description of impurity states for these experiments.

3.2. Hall conductance

In solid state experiments, it is now a standard method to measure the Hall conductance by a four terminal strip. In a cold atom setting, in general, such methods are unavailable as there is no way to make contacts to the cold atom system. One way to overcome this difficulty is to make a scattering type of measurement by letting the cold atom cloud oscillate in a shallow external trap [51]. However, as far as the quantized Hall conductances are concerned, it has been shown that measuring the response of the density of the system to the external magnetic field yields a direct measurement of the Hall conductance by virtue of the Streda formula [52]. Thus, in both cases the effects of impurities on the conductance should be experimentally accessible. Hence, it is important to calculate the Hall conductance in an impure system to understand these experiments.

The Hall conductance of the square lattice over all energy values whose range is given by the Hofstadter butterfly can be calculated by using the Kubo formula [2] for a single value of $\phi/\phi_0 = p/q$,

$$\sigma_{xy} = \frac{e^2}{A_0\hbar} \sum_{E_\alpha < E_f} \sum_{E_\beta > E_f} \times \frac{(\partial\hat{H}/\partial k_1)_{\alpha\beta}(\partial\hat{H}/\partial k_2)_{\beta\alpha} - (\partial\hat{H}/\partial k_2)_{\alpha\beta}(\partial\hat{H}/\partial k_1)_{\beta\alpha}}{(E_\alpha - E_\beta)^2}, \tag{10}$$

where the velocity operators are defined as the partial derivatives of the Hamiltonian with respect to the wave vectors. In addition to two summations for the energy eigenvalues smaller than and greater than the fixed Fermi energy respectively, there is another implied summation over the whole magnetic Brillouin zone. Although the Hall conductance in a gap for a pure system can be calculated via the Diophantine equation which results in the famous TKNN integers [2], in the impurity case the calculation does not simplify to a Diophantine equation. Therefore we calculate the Hall conductance explicitly through the Kubo formula, equation (10). When the Fermi energy lies within a gap, we find that the Hall conductance is an integer multiple of e^2/h, verifying our numerical procedure. The Kubo formula also allows us to calculate the Hall conductance even when Fermi energy lies within a band.

The sweeping of the Fermi energy is an indirect representation of the potential difference that should be present in the system in order to observe a non-zero conduction. A similar procedure has been carried out for triangular and Kagomé lattices under the influence of a staggered magnetic field, and also for a square lattice with multiorbital interactions [32, 33].

The Hall conductances for various impurity cases are displayed as a set in figure 7. These graphs show the Hall conductances in units of e^2/h, as a function of the Fermi energy for the single value of $\alpha = \phi/\phi_0 = p/q = 13/3$ calculated as above. Again we have the pure case with $t_E = t = 1.0$ labeled by (c), in which we see the usual step like quantized integer Hall conductance. It is symmetric around the Fermi energy $E_{\text{Fermi}} = 0$, and we observe a successive integer sequence of conductance in agreement with the Diophantine equation of the Hofstadter butterfly. When we look at the conductance spectrum in (b), where t_E is set to $t_E = 0.25$, we see a deformed conductance; however, we can

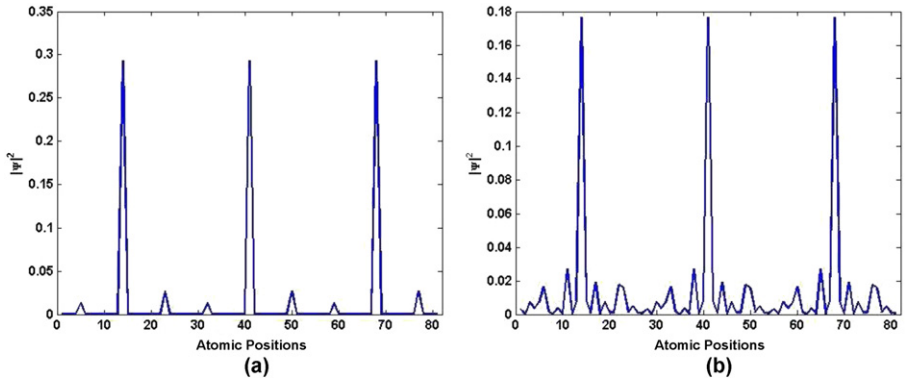

Figure 8. $|\psi|^2$ plots of the localized state wavefunction as a function of the atomic positions of the atoms whose labels are within the boundaries of the magnetic unit cell. The first plot is for the atom 'E' which is close to being a vacancy, i.e. $t_E = 0.005$. The Dirac delta like shaped peaks correspond to the positions of the atom 'E'. Since $q = 3$, there are nine atoms with label 'E' in the magnetic unit cell. The second one has $t_E = 0.50$. As the hopping constant increases, the wavefunction expands more among the other atoms.

see the constant conduction Hall plateaus around $E_{\text{Fermi}} = 0$. We observe new Hall plateaus with Hall conductance $\sigma_{xy} = 0$ centered at $E_{\text{Fermi}} = \pm 0.5$ which are within the dome shaped gaps discussed in the Hofstadter spectrum. For the case of $t_E = 0.001$, figure 7(a), we see that the $\pm e^2/h$ conductance plateaus for $E_{\text{Fermi}} = \pm 0.5$ are narrowed down as the dome shapes become more elliptic. Under these circumstances, a vacancy or an impurity with a smaller hopping constant in the unit cell bears new states that are highly localized on the defect atom. These localized states cannot contribute to the conduction significantly. By setting the hopping parameter of the atom 'E' to a value smaller than the rest of the atoms in the unit cell, we are disabling (or blocking for the vacancy case) the hopping of the electrons through this defect atom. The norm of representative wavefunctions of $E = 0$ energy is plotted through a cut through the magnetic unit cell in figure 8. The two plots for $t_E = 0.005$ and $t_E = 0.50$ demonstrate the localization of the impurity states as t_E is decreased. We see that the wavefunctions are highly localized on the point defect. When the impurity is strongly coupled, i.e. $t_E = 1.50$, the main change in the spectrum is observed near the extremal energies due to the presence of new gaps. These impurity gaps have Hall conductance $\pm e^2/h$ as shown in figure 7(d). We can infer that an impurity atom with higher hopping constant interacts more with the neighboring atoms creating a delocalized impurity state as a result of which new constant conductance Hall plateaus are created.

The Hall conductances for different impurity scenarios in the presence of next nearest neighbor interactions are given in figure 9. The Hall conductance spectra are no longer symmetric around $E_{\text{Fermi}} = 0$, as the bipartite symmetry is broken. The widths of the gaps are now changed, when we look at the energy spectrum along a vertical line which has $\alpha = p/q = 13/3$. Second order interactions do not change the nature of the impurity states. They are highly localized and do not contribute significantly to the conductance. Similarly, for an impurity atom with a high hopping constant, the new conduction plateaus with conductance $\pm e^2/h$ are also robust with respect to the next nearest neighbor hopping. When the magnetic bands of the Hofstadter butterfly are extremely narrow, our direct calculation through the Kubo formula requires extremely fine k-point meshing. Thus, in regions with many small gaps, our results show scattered values for the conduction. However, such fine meshes are not required for the calculation of the conduction within large gaps or for impurity states.

4. Conclusions

The effects of point defects for a square lattice under a magnetic field were investigated. We examined the changes in both the Hofstadter butterfly spectrum and the Hall conductance in detail, considering the first and second order interactions. In order to work with reasonable concentrations of imperfections, we enlarged our unit cell. We proposed a method which provides efficient construction of the A_m matrix through the unit cell geometry. Within our enlarged unit cell, we labeled one of the atoms as an impurity or vacancy, by tuning the hopping constant of that atom to its neighbors. We calculated the energy eigenvalues forming the Hofstadter butterflies, through which we could inspect the effect of these imperfections on the energy spectrum. We also calculated the Hall conductances for different cases of hopping constants, by using the Kubo formalism. For the impurity case, we investigated two different regimes for the hopping constant of the defect atom. The first one was the smaller hopping constant regime, which creates new gaps and bands near the $E = 0$ line of the Hofstadter butterfly. The states which are responsible for these new formations are highly localized and within the newly created gaps the Hall conductance is zero. The second regime was the high hopping constant regime; again the energy spectrum is modified through the creation of new gaps and bands. However, for this case, the impurity atom brings out new Hall plateaus near the extremal energies of the spectrum. We also concluded that the high order interactions, while breaking the symmetry of the butterfly, do not qualitatively change the properties of the impurity states or bands and gaps associated with them.

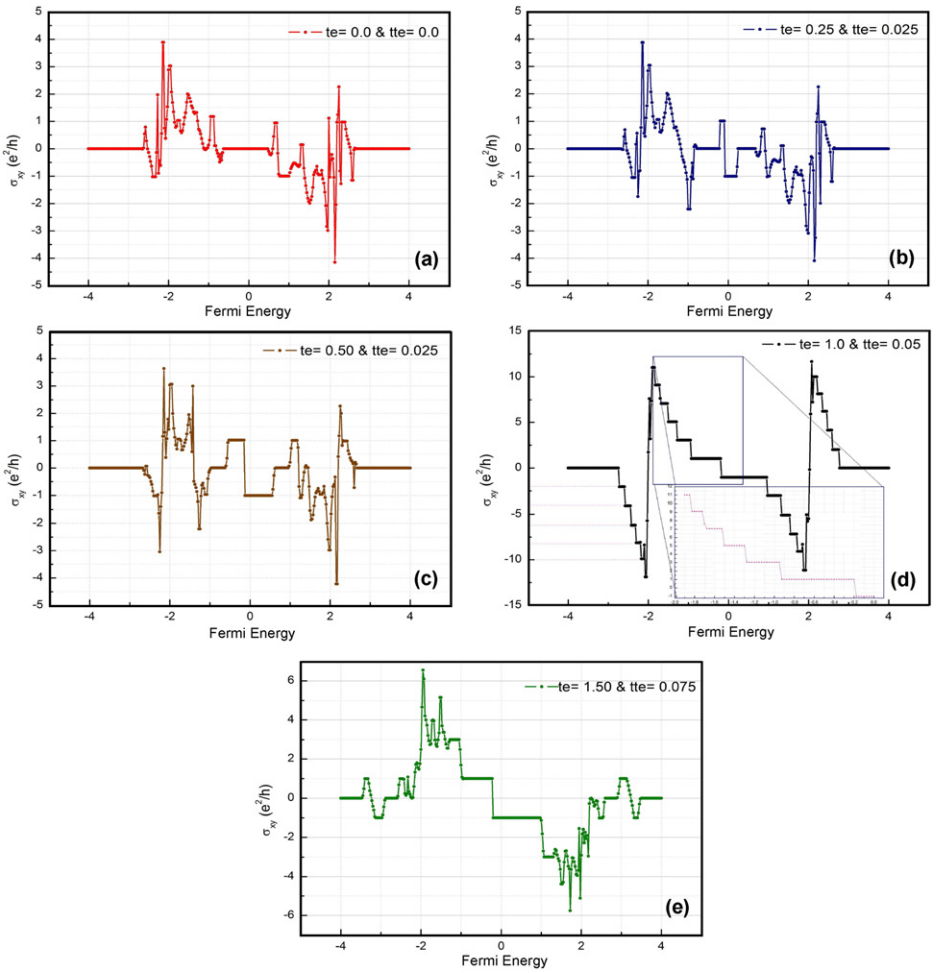

Figure 9. Hall conductivities (in units of e^2/h) as a function of the Fermi energy (in units of 't') with second order interactions where α is set to $p/q = 13/3$: (a) 'E' is a vacancy with $t_{\rm E} = 0.0$ and $tt_{\rm E} = 0.0$; (b) 'E' is an impurity with $t_{\rm E} = 0.25$ and $tt_{\rm E} = 0.025$; (c) 'E' is an impurity with $t_{\rm E} = 0.50$ and $tt_{\rm E} = 0.025$; (d) all of the atoms are the same with $t_{\rm E} = t = 1.00$ and $tt_{\rm E} = tt = 0.050$; the inset shows a zoom in of the region of the spectrum enclosed by a rectangle; (e) 'E' is an impurity with $t_{\rm E} = 1.50$ and $tt_{\rm E} = 0.075$.

Acknowledgments

MOO acknowledges the support from TÜBİTAK, the Scientific and Technological Research Council of Turkey (Grant No. TBAG 109T267). OG acknowledges the support of the Turkish Academy of Sciences, TÜBA.

References

[1] Hofstadter D R 1976 *Phys. Rev.* B **14** 2239
[2] Thouless D J, Kohmoto M, Nightingale M P and den Nijs M 1982 *Phys. Rev. Lett.* **49** 405
[3] Levy N, Burke S A, Meaker K L, Panlasigui M, Zettl A, Guinea F, Castro Neto A H and Crommie M F 2010 *Science* **329** 544
[4] Lin Y-J, Compton R L, Perry A R, Phillips W D, Porto J V and Spielman I B 2009 *Phys. Rev. Lett.* **102** 130401
[5] Lin Y-J, Compton R L, Jiménez-García K, Porto J V and Spielman I B 2009 *Nature* **462** 628
[6] Aidelsburger M, Atala M, Nascimbène S, Trotzky S, Chen Y-A and Bloch I 2011 *Phys. Rev. Lett.* **107** 255301
[7] Jiménez-García K, LeBlanc L J, Williams R A, Beeler M C, Perry A R and Spielman I B 2012 arXiv:1201.6630v1 [cond-mat.quant-gas]
[8] Peierls R 1933 *Z. Phys.* **80** 763
[9] Onsager L 1952 *Phil. Mag.* **43** 1006
[10] Rauh A, Wannier G H and Obermair G 1974 *Phys. Status Solidi* b **63** 215
[11] Azbel M Y 1964 *Sov. Phys.—JETP* **19** 634
[12] Claro F H and Wannier G H 1979 *Phys. Rev.* B **19** 6068
[13] Claro F H 1981 *Phys. Status Solidi* b **104** K31
[14] Zak J 1991 *Phys. Rev. Lett.* **67** 2565
[15] Brown E 1964 *Phys. Rev.* **133** A1038
[16] Gumbs G, Meissein D and Huang D 1995 *Phys. Rev.* B **52** 14755
[17] Bending S J, von Klitzing K and Ploog K 1990 *Phys. Rev. Lett.* **65** 1060
Bending S J, von Klitzing K and Ploog K 1990 *Phys. Rev.* B **42** 9859
[18] Xue D P and Xiao G 1992 *Phys. Rev.* B **45** 5986
Wu X and Ulloa S E 1993 *Phys. Rev.* B **47** 7182
Yagi R and Iye Y 1993 *J. Phys. Soc. Japan* **62** 1279
Chang M C and Niu Q 1994 *Phys. Rev.* B **50** 10843
[19] Hasewaga Y, Hatsugai Y, Kohmoto M and Montambaux G 1990 *Phys. Rev.* B **41** 9174
[20] Gumbs G and Fekete P 1997 *Phys. Rev.* B **56** 3787
[21] Hou J-M and Yang W-X 2009 *Phys. Lett.* A **373** 2774
[22] Rammal R 1985 *J. Phys. (Paris)* **46** 1345
[23] Nemec N and Cuniberti G 2006 *Phys. Rev.* B **74** 165411
[24] İslamoğlu S, Oktel M Ö and Gülseren O 2012 *Phys. Rev.* B **85** 235414

[25] Weiss D, Menschig A, von Klitzing K and Weimann G 1992 *Surf. Sci.* **263** 314
[26] Pfannkuche D and Gerhardts R R 1992 *Phys. Rev.* B **46** 12606
Gerhardts R R and Pfannkuche D 1992 *Surf. Sci.* **263** 324–9
[27] Gerhardts R R, Weiss D and Wulf U 1991 *Phys. Rev.* B **43** 5192
[28] Kohmoto M 1985 *Ann. Phys., NY* **160** 343
[29] Streda P 1982 *J. Phys. C: Solid State Phys.* **15** L717
[30] Albrecht C, Smet J H, von Klitzing K, Weiss D, Umansky V and Schweizer H 2001 *Phys. Rev. Lett.* **86** 147
[31] Analytis J G, Blundell S J and Ardavan A 2004 *Am. J. Phys.* **72** 613
[32] Li J, Wang Y-F and Gong C-D 2011 *J. Phys.: Condens. Matter* **23** 156002
[33] Wang Y-F and Gong C-D 2010 *Phys. Rev.* B **82** 113304
[34] Hasegewa Y and Kohmoto M 2006 *Phys. Rev.* B **74** 155415
[35] Geisel T, Ketzmerick R and Petschel G 1991 *Phys. Rev. Lett.* **66** 1651
Geisel T, Ketzmeric R and Petschel G 1995 *Quantum Chaos* ed G Casati and B Chirikov (Cambridge: Cambridge University Press)
[36] Schlösser T, Ensslin K, Kotthaus J P and Holland M 1996 *Europhys. Lett.* **33** 683
[37] Gudmundsson V and Gerhardts R R 1996 *Phys. Rev.* B **54** R5223
[38] Kuhl U and Stöckmann H-J 1998 *Phys. Rev. Lett.* **80** 3232
[39] Richoux O and Pagneux V 2002 *Europhys. Lett.* **59** 34
[40] Kuhl U, Barkhofen S, Tudorovskiy T, Stöckmann H-J, Hossain T, de Forges de Parny L and Mortessagne F 2010 *Phys. Rev.* B **82** 094308
[41] Ott H, de Mirandes E, Ferlaino F, Roati G, Modugno G and Inguscio M 2004 *Phys. Rev. Lett.* **92** 160601
[42] Zimmermann B, Müller T, Meineke J, Esslinger T and Moritz H 2011 *New J. Phys.* **13** 043007
[43] Tarruell L, Greif D, Uehlinger T, Jotzu G and Esslinger T 2012 *Nature* **483** 302
[44] Hatsugai Y 1993 *Phys. Rev. Lett.* **71** 3697
[45] Kohmoto M 1989 *Phys. Rev.* B **39** 11943
[46] Goldman N 2009 *J. Phys. B: At. Mol. Opt. Phys.* **42** 055302
[47] Hatsugai Y and Kohmoto M 1990 *Phys. Rev.* B **42** 8282
[48] Van de Walle C G and Neugebauer J 2004 *J. Appl. Phys.* **95** 3851
[49] Harper P G 1955 *Proc. Phys. Soc.* A **68** 874
[50] Abrahams E, Anderson P W, Licciardello D C and Ramakrishnan T V 1979 *Phys. Rev. Lett.* **42** 673
[51] LeBlanc L J, Jiménez-García K, Williams R A, Beeler M C, Perry A R, Phillips W D and Spielman I B 2012 arXiv:1201.5857v1 [cond-mat.quant-gas]
[52] Umucalılar R O, Zhai H and Oktel M Ö 2008 *Phys. Rev. Lett.* **100** 070402